Microstructural and Biochemical Characterization of the Nano-porous Sucker Rings from *Dosidicus gigas***

By *Ali Miserez, James C. Weaver, Peter B. Pedersen, Todd Schneeberk, Roger T. Hanlon, David Kisailus*, Henrik Birkedal**

Dr. Ali Miserez
Materials Department and Department of Molecular, Cellular, and Developmental Biology
University of California, Santa Barbara
Santa Barbara, CA-931066-5050 (USA)

Prof. David Kisailus and Dr. James C. Weaver
Department of Chemical and Environmental Engineering
University of California, Riverside
CA 92521 (USA)
Email: david@engr.ucr.edu

Prof. Henrik Birkedal and B.Sc. Peter B. Pedersen
Department of Chemistry and Interdisciplinary Nanoscience Center, University of Aarhus
140 Langelandsgade
DK-8000 Århus C (Denmark)
Email: hbirkedal@chem.au.dk

Todd Schneeberk
Department of Molecular, Cellular, and Developmental Biology
University of California, Santa Barbara
Santa Barbara CA 93106 (USA)

Dr. Roger T. Hanlon
Marine Biological Laboratory
Woods Hole, MA 02543 (USA)

*Corresponding Authors

**We thank J. Herbert Waite and Amy Butros for helpful suggestions, the crew of the *Coroloma* (Ventura Harbor, CA, USA) for their assistance in specimen collection and R. Imondi and L. Santschi from *Coastal Marine Biolabs* (Ventura Harbor, CA, USA) for help with sample preparation. We thank MAXLAB for access to synchrotron radiation. We gratefully acknowledge funding from the Swiss National Science Foundation (AM, PA002–113176 / 1), NIH 5 R01 DE 014672, DANSYNC for supporting the synchrotron experiments, and the Danish Research Councils, as well as partial support (RTH) by DARPA DSO BioDynotics Program (Project N66001-03-C-8043). AM and JCW contributed equally to this work.

Keywords: Cephalopoda, Proteinaceous, Cellular Solids, Biomimetic

Recent interest in the development of environmentally benign routes to the synthesis of novel multifunctional materials has resulted in numerous investigations into structure-function relationships of a wide range of biological systems at the ultrastructural, micromechanical, and biochemical levels.[1]. While much of this research has concentrated on mineralized structures such as bone,[2-4] mollusk shells[5-7] sponge spicules[8-11] and echinoderm ossicles,[12-15] there is an equally broad range of animals whose skeletal structures are devoid of mineral components.[16-18] One such group, the squids (Mollusca: Cephalopoda: Teuthoidea), are remarkable in several aspects. In addition to having an exceptionally well developed brain, sensory systems and skin (for adaptive coloration)[19], these swift agile predators[20] have eight flexible strong arms, two fast extensible tentacles, and strong malleable suckers, all of which are muscular hydrostats[21].

Squid possess four extracellular hard tissues that are crucial for their survival: (i) the pen, which acts as a rod-like reinforcing structure of the long body mantle; (ii) the beak, situated at the anterior extremity of the digestive system, enveloped by the buccal mass, which is used for prey dismemberment; (iii) the cartilaginous cranium protecting the central nervous system (CNS), and (iv) the sucker rings, ring-like structures within the suckers that provide additional gripping power during prey capture and handling.

Previous studies have revealed the structural characteristics and chemical composition of the first two: the pen is mainly composed of β-chitin,[22,23] while the beak is a graded composite structure composed of α-chitin[24-26] and heavily cross-linked proteins with various degrees of hydration.[27] Structural, mechanical, and biochemical data of the sucker rings, however, are lacking. Given their specific mechanical function

for increasing gripping capacity and their rigid, wholly organic composition, it is thus of interest from a materials perspective to elucidate the relationships between those properties, their function, and their biochemistry.

The species used in this study, the Humboldt squid, *Dosidicus gigas*, is a large, aggressive and predatory species commonly encountered throughout the Eastern Pacific. They can reach lengths of nearly 2 m and a mass up to 50 kg. In this species, each of the eight arms and two tentacles is lined with suckers that contain an interior rigid ring equipped with formidable triangular teeth (Fig. 1). The presence of the sucker rings increases the functionality of the suckers, most likely by reducing the shear forces (created by struggling prey) that could break the seal created by the infundibulum of the sucker. As the circular muscles of each sucker contract, the teeth are bent inward and subsequently penetrate the skin or scales of strong fast prey such as fishes. The sucker ring teeth are very sharp, and even moderately sized *Dosidicus gigas* (1 m total length) can easily lacerate a human arm (personal – and painful – observation by a coauthor).

Each sucker ring consists of a basal ring and a series of dentitions (Fig. 1C). SEM images of fracture surfaces reveal that they are composed of a series of parallel tubular elements (Fig. 2). The channels [with an average diameter of 215 +/- 60 nm (n=775)] are orientated parallel to the dentitions and then spread out through the basal ring as indicated in Fig. 2A. Towards the surface of the sucker ring, the channels are filled and the surface lacks any detectable porosity.

Closer examination of the channel organization reveals that the pore fraction across a given tooth is not uniform and that there is a gradual decrease in pore fraction from the tooth core to the periphery. This is accomplished through both reduction in

channel diameter and increase of channel spacing. The dependence of the channel diameter on distance from the tooth edge is shown in Fig. 2F. The channel diameter increases gradually from around 100 nm close to the surface and reaches over 99% of the maximum values (259 nm) at a distance from the surface equivalent to approximately 20% of the tooth diameter (derived from a fit of a sigmoidal growth curve to the data). There is also a concomitant decrease in channel spacing, resulting in a corresponding increase in void fraction from <2% near the periphery to ca. 20% near tooth core as shown in Fig. 2G. The channels do not display any long-range lateral ordering (e.g. hexagonal), Fig. 2D. Not surprisingly, there is a positive linear correlation (correlation coefficient, $R = 0.626$) between the pore diameter and the nearest neighbor distance. The average inter-channel nearest neighbor distance was 343±76 nm, while the next nearest and second nearest neighbor distances were 443±95 and 585±156 nm, respectively.

The parallel channel-like ultrastructural organization of the sucker rings has a direct effect on their mechanical properties, which were investigated via nanoindentation. Because of the exposed nature of the sucker ring teeth (the basal ring is largely protected within the sucker musculature – cf. Fig. 1B) and their direct mechanical loading during prey capture and handling, they were the primary focus of the mechanical studies described below. Typical cross-sectional modulus and hardness maps through the sucker ring teeth are presented in Fig. 3. When examined in the dry state, there is a distinctive gradient of decreasing modulus (E_e) and hardness (H_e) from the tooth periphery to the core. Peak modulus and hardness values near the tooth periphery are ca. 7-7.5 GPa and 0.7 GPa, respectively, while in the tooth core reach minimum values of ca. 4.5-5 GPa and 0.4 GPa, respectively, *i.e.* an E_p/E_e ratio of 0.65. Hydrated samples exhibit similar trends,

even though the modulus and hardness differences between the tooth periphery and core are less pronounced. The modulus ranges between 2.75 (periphery) to 1.75 (core) GPa, and the hardness between 0.25 and 0.15 GPa. Overall, one notices a 2.5 to 3-fold decrease in both E and H in a given region for hydrated sections compared to dry ones. However, swelling during hydration, which would subsequently lead to a modified mechanical response, cannot be ruled out.

The porous structure of the sucker rings is reminiscent of wood[28], in that it contains elongated cellular pores running in a preferred orientation within the tissue. For these types of cellular structures the variation in modulus as a function of pore fraction V_p can be estimated using equations for idealized honeycomb structures:

$$E_p \approx E_s \cdot \left(\frac{C_1 - V_p}{C_1} \right)^m \qquad (1)$$

where E_p is the modulus of the porous network, E_s is the modulus of the solid material, C_1 is a constant close to unity and m is a factor that accounts for the effect of the loading direction relative to the tubule orientation. When loading along the axis of the tubules, the major deformation mechanism is wall stretching or compression (at low strains) and the decrease in modulus with porosity content is essentially linear ($m = 1$). For off-axis loading (*i.e*. perpendicular to the axis of the tubules), deformation is dominated by wall bending, a much more compliant deformation mode that results in a cubic-law decrease of modulus with porosity ($m = 3$).

Quantitative analysis of SEM images showed that V_p in the sucker ring teeth varies from 1.6 (V_e) to 21% from the periphery to the core. Rewriting Eq. 1 to account for the fine porosity of the tooth periphery, one obtains a ratio E_p/E_e given by:

$$\frac{E_p}{E_e} \approx \left(\frac{C_1 - V_p}{C_1 - V_e} \right)^m \qquad (2)$$

where V_e is the pore volume fraction of the tooth periphery, and E_e is the modulus at the periphery. A plot of Eq. 2 for the two limiting cases (parallel and perpendicular to the tubule axis) is shown in Fig. 3C, and indicates that the corresponding ratio of E_p/E_e ranges between 1 and 0.82 for loading along the axis, and 1 to 0.54 for loading perpendicular to the tubule axis. Experimentally, the measured range of E_p/E_e was between 1 and 0.65. During the nanoindentation experiments, the exact orientation of the tubules relative to the surface, θ, was unknown and depends on the distance of the cutting plane from the tooth tip, and on the cutting plane angle (Figs. 2A and 3A). The modulus response will then be bounded by the two limiting cases. Assuming a simple rule-of-mixture for the modulus as a function of θ, $(E_p/E_e)_\theta$, we may write:

$$\left(E_p/E_e\right)_\theta = \left(E_p/E_e\right)_0 \cos^2(\theta) + \left(E_p/E_e\right)_{90} \sin^2(\theta) \qquad (3)$$

where $(E_p/E_e)_0$ and $(E_p/E_e)_{90}$ are the relative moduli for loading perpendicular and parallel to the tubule direction, respectively. Using Eq. 3, we find that the predicted range of moduli for a 45° angle surface/tubule orientation is close to that measured experimentally, as also plotted in Fig. 3C. Although more work is necessary to further quantify the influence of pore orientation and geometry, this analysis, in conjunction with results obtained from elemental and biochemical characterization of the sucker rings (which revealed no distinct chemical gradients, see below), suggests that the observed differences in mechanical properties are likely due to structural (porosity) rather than biochemical gradients.

The presence of a porous (cellular) architecture is a well-documented feature in a

variety of natural materials, such as wood, trabecular bone, and plant stems.[29] Their common design of a porous core supporting a denser periphery results in a high specific bending stiffness (bending stiffness normalized to material density). However, the pore volume fraction is typically much higher (80-90%) than in the sucker rings, which are ca. 20%. In addition, because the total weight of the sucker rings compared to that of the remainder of the animal is negligible, it is doubtful that the porous structure observed here is adapted for weight reduction. The orientation of the channels that run parallel to the long axis of the teeth probably increase their bending stiffness, a feature that is most important where they are likely to be subjected to large bending or shear forces because the suckers themselves are soft actuators that flex in many directions. In addition, the graded hardness (*i.e.*, harder at the tooth edge, and progressively softer towards the tooth interior) resulting from the porosity gradient is a micromechanical feature recently observed in several structural biological materials that must exhibit a high wear tolerance due to their direct contact with the external environment.[17, 30, 31] An additional advantage of the porous architecture is to reduce the probability of catastrophic structural failure by introducing a potential crack-arresting mechanism at the boundaries between the two constituent materials (in this case protein and seawater). As has been described for crack propagation in wood, the presence of the channel-like architecture in the sucker rings likely results in significant energy dissipation as a propagating crack follows a non-linear progression through the material,[28] as is commonly observed in fractured tooth surfaces (Fig. 2B).

Elemental analysis via energy dispersive X-ray spectroscopy (EDS) revealed (in addition to C, N, and O), the presence of a uniform distribution of both Cl and S

throughout the sucker rings, although no metals were detected (Fig. 4A). In addition to the lack of mineralization, position resolved wide-angle x-ray scattering experiments showed that the sucker rings also lack any semicrystalline organic constituents. The latter observation makes it unlikely that chitin, a common biological structural polysaccharide, is present. This was further confirmed during amino acid analysis where chitin (or chitosan) is detected from the hydrolysis product, glucosamine.[24] No chitin was detected (Fig. 4B). This is surprising considering that chitin makes up about 15-20 wt.% of the beak tip and is the dominant structural material of the pen in *Dosidicus gigas*[22,23].

Complete amino acid compositional analysis of the sucker rings reveal a high Gly (37 mole %), Tyr (14 mole %) and His (13 mole %) content (Fig. 4C), which was further confirmed following electrophoretic separation of the sucker ring proteins and cross-reactivity with the His-specific Pauly's stain (Fig. 4D). This distinctive amino acid composition is a notable feature given the recurring presence of Gly- and His-rich proteins in load-bearing and impact-resistant tissues.[32] In such structures, the imidazole side-chain has been shown to be particularly versatile in its ability to couple with various chemical entities. This can be in the form of coordination bonds with transition metals (as in the jaws of *Nereis*, a predatory marine worm)[33-35] or as covalent cross-links with peptidyl dihydroxy phenylalanine (DOPA) in squid beaks.[27] In yet another predatory marine worm (*Glycera*), His-rich proteins coexist with a complex composite structure of melanin, Cu ions, and atacamite mineral[16, 34, 36, 37] although the nature of the imidazole side chain interactions at the molecular level have yet to be characterized. Although it is tempting to attribute the mechanical robustness of the sucker rings to the high His content, none of the aforementioned components were detected; metal ions, mineral,

DOPA, and melanin are all absent in the sucker rings. Significantly, the rigidity of the sucker rings decreases with increasing water temperature, becoming noticeably pliable at temperatures as low as 10ºC over ambient, suggesting that structural stabilization is predominantly through hydrogen bonding. This is further supported by the observations that the sucker rings completely dissolve in concentrated formic acid, a known disrupter of hydrogen bonding interactions[38] and that the heat-induced pliability is a reversible phenomenon. We thus suggest that His residues take part in forming a stable hydrogen bonded network. The large quantities of Tyr could be related to sclerotization, which would also help explain the brown coloration in the sucker rings. It is likely that Tyr and possibly also His are partially chlorinated as has been observed in *Neries* worm jaws.[33] Another remarkable feature of the amino acid composition of these squid rings is the large abundance of hydrophobic amino acids other than Tyr (25.5% total for Leu, Ala, Val, Phe, Ile, Met). Hence hydrophobic interactions can be expected to play an additional stabilizing role for the sucker rings.

As revealed from these studies, the chlorinated, wholly proteinaceous sucker rings of *Dosidicus gigas* exhibit a unique set of characteristics not reported previously for any other biological structural material. They consist of a nanoscale network of parallel tubular elements that are presumably stabilized almost entirely by hydrogen bonding and hydrophobic interactions. It is remarkable that the sucker rings do not contain chitin, which is common in mollusks and is an integral part of the pen and beak of squids.[24] The mechanical properties can be understood from the porous nature of the ring material suggesting that microstructural characteristics (variation in pore fraction) rather than

biochemical or elemental gradients are primarily responsible for the localized differences in mechanical response.

Experimental

Humboldt squid, *Dosidicus gigas*, collected from Hueneme Canyon (N 34.06, W 119.16) from May-July, 2007 at depths ranging from 110 m to 183 m, were used in this study. The sucker rings, isolated from 10 individuals, were soaked overnight in deionized water to remove residual salt. The sucker rings were then air dried, mounted on aluminum stubs using conductive carbon tape and examined by Scanning Electron Microscopy (SEM) and Energy Dispersive Spectroscopy (EDS). Additional sucker rings were fractured and prepared as described above. Analysis of pore size, inter-pore distances and pore fractions were determined using Photoshop (Adobe) followed by further statistical treatment in Origin (OriginLab, Northampton, MA, USA) combined with home written programs. In total, more than 50 sucker rings were examined and the results presented are representative of the trends observed.

Position resolved X-ray diffraction measurements were performed at beam line ID-711 at the MAX-III synchrotron in Lund, Sweden with a MARCCD detector and a lateral resolution defined by the beam size of 0.4×0.4 mm. Analyses were performed on both the dentitions (teeth) and the basal ring. No diffraction was detected anywhere in the samples. Ground samples were also investigated with powder diffraction using Cu $K\alpha$ radiation; no diffraction was observed.

Elastic modulus (E) and hardness (H) of sucker rings were obtained by probing flat surfaces by nanoindentation, using a Triboindenter (Hysitron, Minneapolis, MN, USA)

equipped with a 30 mN load transducer. Full sucker rings or isolated individual teeth were embedded in Epofix resin. Flat and smooth surfaces were subsequently obtained by ultra-microtomy (Leica EM UC6, Leica Mikrosysteme GmbH, Wetzlar, Germany), using fine cutting conditions (80 nm thick sections at a speed rate of 1 mm/sec). In a typical sample preparation, 4 to 8 teeth were revealed on fresh sucker ring cross-section surfaces, while other sections were also made in the longitudinal direction. Microtomed sections were placed into a custom-made glass fluid cell and placed inside the indenter chamber. An elongated 90° cube-corner tip was employed, allowing measurements in both dry and wet conditions. Indents were placed according to grids that completely covered the entire tooth cross-sections, with lateral size of the indent grids ranging from 150 to 400 µm depending on the location (and thus dimensions) of the tooth section. Indentation conditions were chosen so as to minimize visco-elastic effects, using a peak load of 2000 µN, a loading/unloading rate of 200 µN/s, and a holding time at peak load of 10 s. Following the dry condition, the cell was subsequently filled with water until the sample was fully submerged, and the system was stabilized for at least one hour. Identical indent grid patterns were applied, with a 5 µm offset to avoid indentation overlapping. The hydrated surface was probed using the same experimental conditions. Load-displacement curves were analyzed for *E* and *H* according to the Oliver and Pharr method.[39] Property contour maps were generated using the Origin graphing software (OriginLab, Northampton, MA, USA).

Amino acid composition was measured on a Ninhydrin-based Beckman autoanalyzer (Beckman-Coulter, Fullerton, CA). Individual sucker rings were freeze-dried, ground to powder with mortar and pestle, weighed, and placed inside hydrolysis

tubes for 2 or 24 h treatments. Hydrolysis was carried out *in vacuo* at 110°C in 6 N HCl / 5% phenol solution. The hydrolysate was then flash-evaporated, thoroughly washed, and re-suspended in buffer. A volume of 100 µl of the solution was loaded in the analyzer for each specimen. The relative amino acid composition was corrected using external standards. A total of ten sucker rings of various sizes were individually analyzed.

Additional sucker rings were ground to fine powder under liquid nitrogen with a mortar and pestle. Proteins extraction was then performed with 5% acetic acid and 8 M urea. Homogenates were centrifuged, and the supernatant was collected and used for gel electrophoresis.

Routine sodium dodecyl sulfate polyacrylamide gel electrophoresis (SDS-PAGE) was used for protein separation (15% Acrylamide, 1.35% N.N'-methylenebisacrylamide). Parallel lanes were stained with Coomassie blue and the Pauly's solution[40], which specifically stains for His-rich proteins. Prior to Pauly's staining, gels were rinsed in isopropanol and water in order to remove the residual SDS, a prerequisite for the staining technique.

Received: ((will be filled in by the editorial staff))
Revised: ((will be filled in by the editorial staff))
Published online: ((will be filled in by the editorial staff))

[1] M. A. Meyers, P. Y. Chen, A. Y. M. Lin, Y. Seki, *Progress in Materials Science* **2008**, 53, 1.
[2] G. E. Fantner, T. Hassenkam, J. H. Kindt, J. C. Weaver, H. Birkedal, L. Pechenik, J. A. Cutroni, G. A. G. Cidade, G. D. Stucky, D. E. Morse, P. K. Hansma, *Nature Materials* **2005**, 4, 612.
[3] S. Weiner, H. D. Wagner, *Annu. Rev. Mater. Sci*. **1998**, 28, 271.
[4] D. R. Carter, W. C. Hayes, *Journal of Bone and Joint Surgery-American Volume* **1977**, *59*, *7*, 954-962
[5] Z. Tang, N. A. Kotov, S. Magonov, B. Ozturk, *Nature Materials* **2003**, 2, 413.
[6] A. P. Jackson, J. F. V. Vincent, R. M. Turner, *Proceedings of the Royal Society of London Series B-Biological Sciences* **1988**, 234, 1277, 415
[7] R. Z. Wang, Z. Suo, A. G. Evans, N. Yao, I. A. Aksay, *Journal of Materials Research*, **2001**, 16, 9, 2485-2493
[8] J. Aizenberg, J. C. Weaver, M. S. Thanawala, V. C. Sundar, D. E. Morse, P. Fratzl, *Science* **2005**, 309, 275.
[9] J. C. Weaver, J. Aizenberg, G. E. Fantner, D. Kisailus, A. Woesz, P. Allen, K. Fields, M. J. Porter, F. W. Zok, P. K. Hansma, P. Fratzl, D. E. Morse, *Journal of Structural Biology* **2007**, 158, 1, 93-106
[10] A. Miserez, J. C. Weaver, P. J. Thurner, J. Aizenberg, Y. Dauphin, P. Fratzl, D. E. Morse, F. W. Zok, *Advanced Functional Materials* **2008**, 18, 8, 1241-1248
[11] C. Levi, J. L. Barton, C. Guillemet, E. Lebras, P. Lehuede. *Journal of Materials Science* **1989**, 8, 3, 337-339
[12] A. Sidorenko, T. Krupenkin, A. Taylor, P. Fratzl, J. Aizenberg, *Science* **2007**, 315, 487.
[13] J. Aizenberg, A. Tkachenko, S. Weiner, L. Addadi, G. Hendler, *Nature* **2001**, 412, 6849, 819-822
[14] Y. Politi, T. Arad, E. Klein, S. Weiner, L. Addadi, *Science* **2004**, 306,5699, 1161-1164
[15] F. H. Wilt, *Zoological Science*, **2002**, 19, 3, 253-261
[16] H. C. Lichtenegger, H. Birkedal, J. H. Waite, in *Metal Ions in Life Sciences*, Vol. 4 (Eds: A. Sigel, H. Sigel, R. K. O. Sigel), Wiley, **2008**, 295.
[17] N. Holten-Andersen, G. E. Fantner, S. Hohlbauch, J. H. Waite, F. W. Zok, *Nature Materials* **2007**, 6, 669.
[18] J. F. V. Vincent, U. G. K. Wegst, *Arthropod Structure & Development* **2004**, 33, 187.
[19] R. T. Hanlon, J. B. Messenger, J.B., *Cephalopod Behaviour*, **1996** Cambridge: Cambridge University Press.
[20] T. Kubodera, K. Mori, *Proc Proc. R. Soc Soc. B*, **2005**, 272, 2583–2586
[21] W. M. Kier, K. K. Smith, *Zoological Journal of the Linneaen Society*, **1985**, 83, 307-324.
[22] S. Hunt, A. El Sherief, *Tissue & Cell* **1990**, 22, 191.
[23] Y. M. Lee, H. K. Kim, S. J. Kim, *Polymer* **1996**, 37, 5897.
[24] A. Miserez, Y. Li, J. H. Waite, F. Zok, *Acta Biomaterialia 2007*, 3, 139.
[25] S. Hunt, M. Nixon, *Comp. Biochem. Physiol*. **1981**, 68B, 535.
[26] C. Jeuniaux, in *Comprehensive Biochemistry*, Vol. 26C (Eds: M. Florkin, E. H. Stotz), Elsevier Publishing Company, Amsterdam, The Netherlands **1971**, 595.

[27] A. Miserez, T. Schneberk, C. Sun, F. W. Zok, J. H. Waite, *Science* **2008**, 319, 1816.
[28] L. J. Gibson, M. F. Ashby, *Cellular Solids: Structure and Properties, 2nd Ed.* **1999** Pergamon Press.
[29] L. J. Gibson, *Journal of Biomechanics* **2005**, 38, 377.
[30] V. Imbeni, J. J. Kruzic, G. W. Marshall, S. J. Marshall, R. O. Ritchie, *Nature Materials* **2005**, 4, 229.
[31] M. G. Pontin, D. N. Moses, J. H. Waite, F. W. Zok, *Proc. Natl. Acad. Sci. USA* **2007**, 104, 13559.
[32] C. C. Broomell, R. K. Khan, D. N. Moses, A. Miserez, M. G. Pontin, G. D. Stucky, F. W. Zok, J. H. Waite, *J. Roy. Soc. Interface* **2007**, 4, 19.
[33] H. Birkedal, R. K. Khan, N. Slack, C. Broomell, H. C. Lichtenegger, F. Zok, G. D. Stucky, J. H. Waite, *ChemBioChem* **2006**, 7, 1392.
[34] H. C. Lichtenegger, T. Schöberl, J. T. Ruokolainen, J. O. Cross, S. M. Heald, H. Birkedal, J. H. Waite, G. D. Stucky, *Proc. Natl. Acad. Sci. USA* **2003**, 100, 9144.
[35] C. Broomell, M. A. Mattoni, F. W. Zok, J. H. Waite, *J. Exp. Biol*. **2006**, 209, 3219.
[36] H. C. Lichtenegger, H. Birkedal, D. M. Casa, J. O. Cross, S. M. Heald, J. H. Waite, G. D. Stucky, *Chem. Mater*. **2005**, 17, 2927.
[37] D. N. Moses, J. H. Harreld, G. D. Stucky, J. H. Waite, *J. Biol. Chem.* **2006**, 281, 34826.
[38] J. F. V. Vincent, *Materials Research Symposium Proceedings* **2006**, 898E.
[39] W. C. Oliver, G. M. Pharr, *J. Mater. Res*. **1992**, 7, 1564.
[40] D. Sahal, R. Kannan, A. Sinha, V. Babbarwal, B.G. Prakash, G. Singh, and V.S. Chauhan, *Anal. Biochem*., **2002**, 405.
[41] W. E. Hoyle, *Report on the Cephalopoda collected by H.M.S. Challenger during the Years 1873-76*. **1886**

Figures:

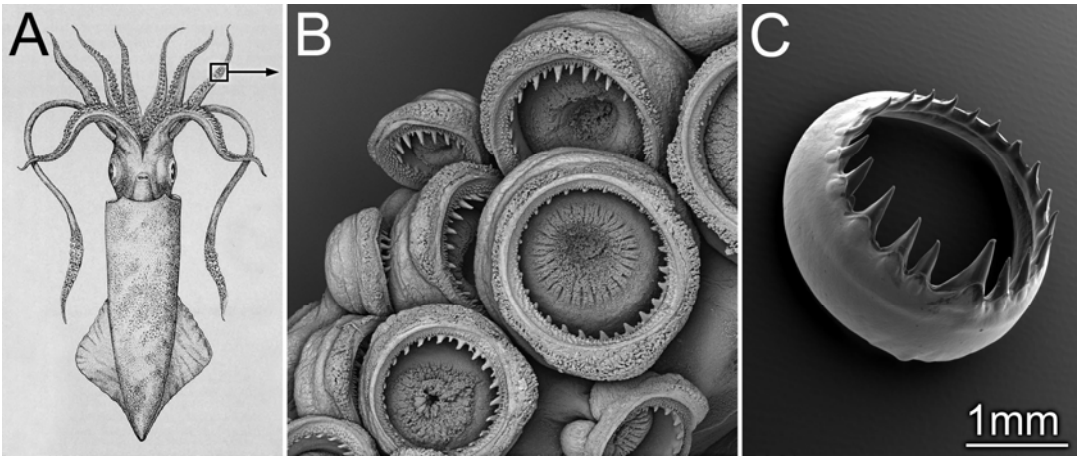

Figure 1. Located along the muscular arms and tentacles of squid (A), and contained within each sucker (B), are the proteinaceous sucker rings (in this case, from the genus *Loligo*). One such sucker ring, isolated from an arm of *Dosidicus gigas*, is shown in (C). The squid illustration in "A" was adapted from [41].

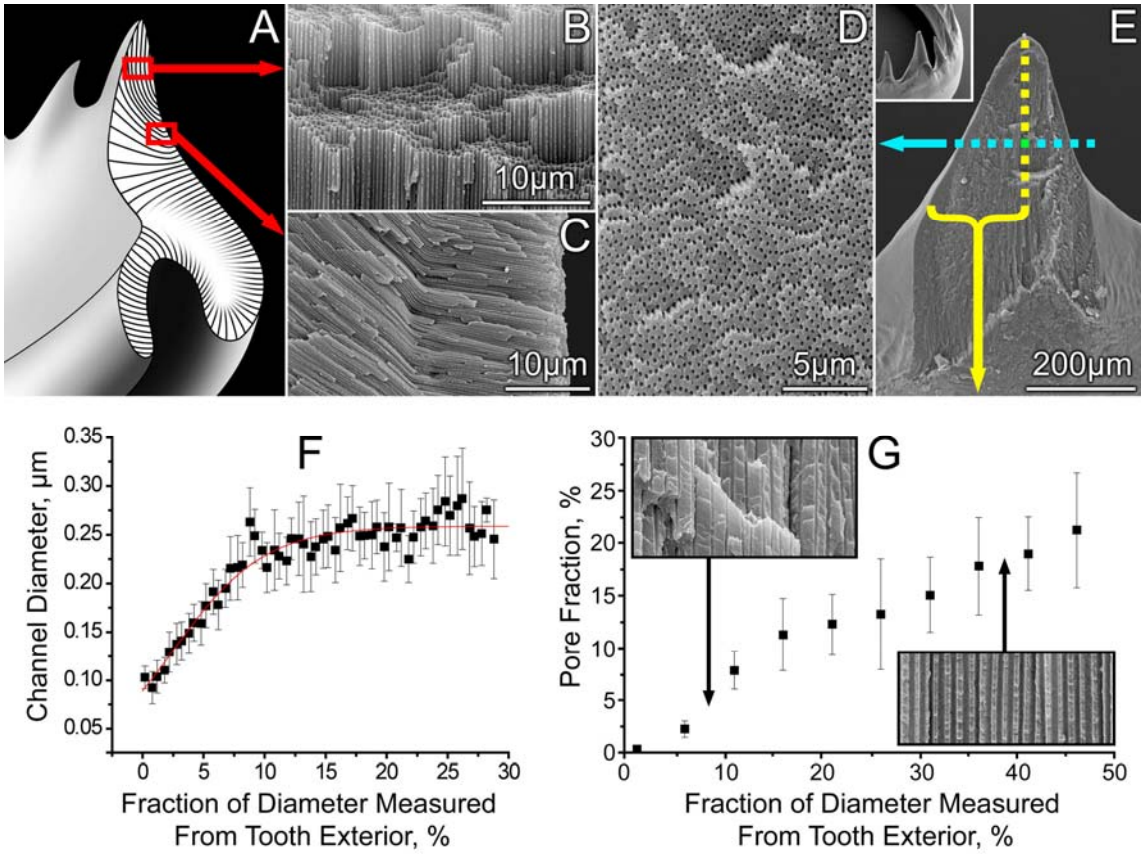

Figure 2. Ultrastructural features of *D. gigas* sucker rings. (A) illustration of a sucker ring cross-section revealing the channel organization extending from a tooth tip down into the basal ring. The two SE micrographs shown in (B) and (C) reveal the highly parallel nature of the fused tubular elements. (D) shows a cross-sectional SE micrograph of a single tooth revealing the relatively uniform local pore diameter and their apparent lack of lateral ordering. (E) shows a longitudinally sectioned tooth and a sample region from which the data presented in (G) were obtained. (F) Pore diameter as a function of distance from edge measured on a transverse cross section through a tooth, a part of which is shown in (D). Error bars are root mean square deviations. The red line represents a fit to a sigmoidal function to the data. (G) Pore fraction as a function of distance from the tooth periphery to the core and includes two representative SE micrographs of tooth longitudinal sections illustrating the changes in both channel diameter and spacing as a function of location.

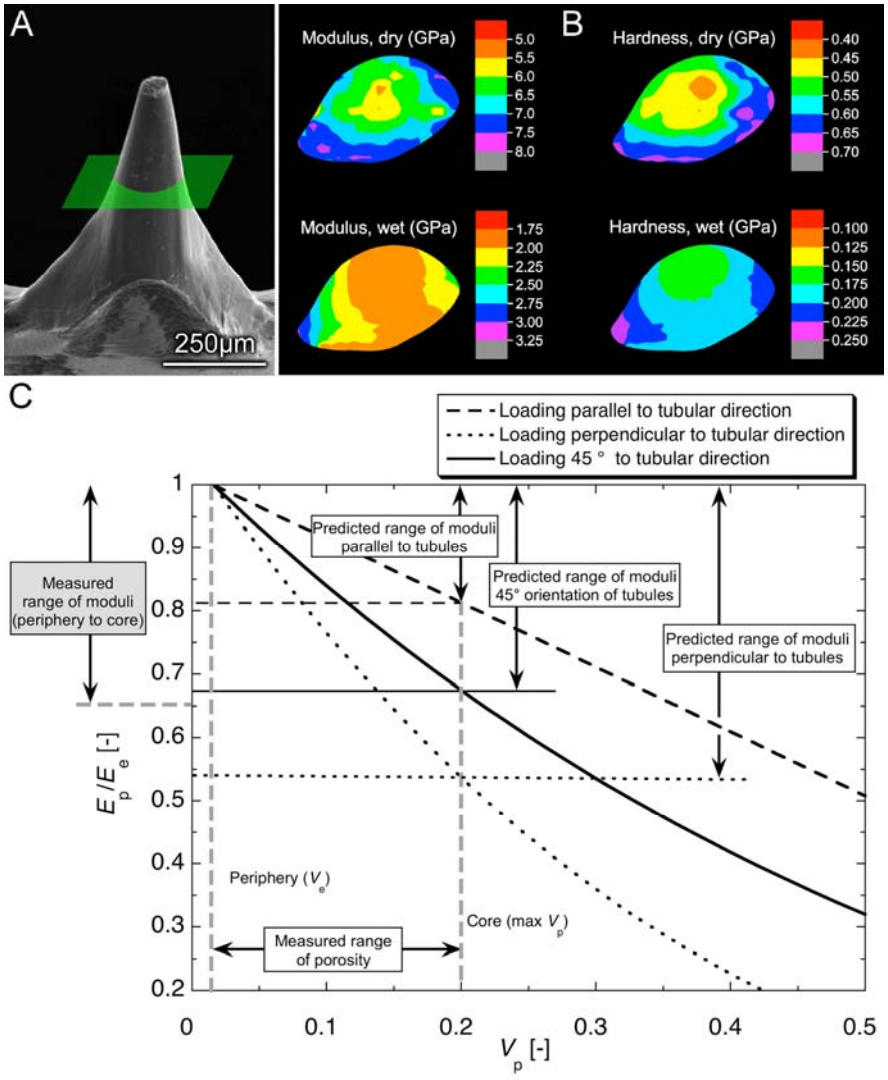

Figure 3. Micromechanical properties measured on cross-sections of sucker ring teeth. (A) Individual tooth and illustration of the microtome cutting plane. (B) Nanoindentation maps of modulus and hardness in dry and wet conditions. The maps were generated from arrays of 300 to 500 indents. (C) Relative modulus E_p/E_e (with E_p, the modulus of the core and E_e, that of the periphery) as a function of pore fraction V_p according to Eq. 2 for cellular materials with an applied load parallel to (dashed line) and perpendicular to (dotted) the tubule axis. The solid line is E_p/E_e as a function of V_p for a surface-to-tubule axis angle of 45° as predicted by Eq. 3. Comparisons of the range of moduli ratio obtained from nanoindentation experiments and those predicted from porosity measurements (SEM micrographs), suggest that the tubules were inclined ca. 45° relative to the loading surface in this sample.

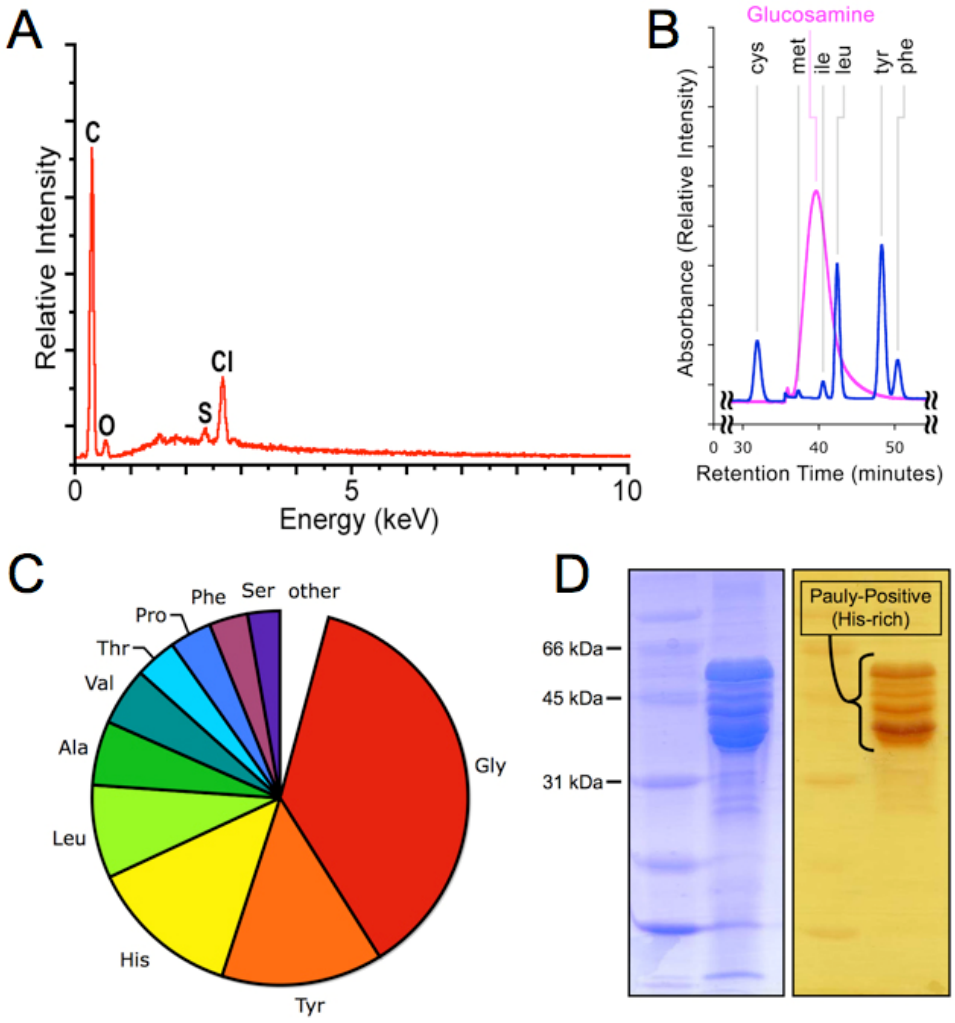

Figure 4. Elemental and chemical composition of the *D. gigas* sucker rings. (A) Energy dispersive X-ray analysis (EDS) reveals the presence of both chlorine and sulfur, but no metals are detected. (B) A portion of the amino acid analysis data (blue curve) showing the region where the acid hydrolysis product of chitin, glucosamine, would be expected compared to a glucosamine standard (pink curve); no chitin is detected. (C) Pie chart showing the relative proportions of specific amino acids in the sucker rings. (D) Gel electrophoresis analysis of sucker ring proteins. Left panel is with Coomassie staining while the right panel is with the His-specific Pauly's stain.